Wang *et al. Animal Diseases* (2025) 5:10
https://doi.org/10.1186/s44149-025-00164-z

Animal Diseases

ORIGINAL ARTICLE

Open Access

DNA aptamers targeting glycoprotein D enable specific detection of pseudorabies virus (PRV)

Zhihao Wang[1], Yan Qiao[1], Jiafu Zhao[1], Xiaotian Chang[1], Heshui Zhu[1,2,3] and Chao Zhang[1,2,3*]

Abstract

Pseudorabies virus (PRV, *SuidAlphaherpesvirus* 1) causes substantial economic losses in swine production. Here, we report the development of DNA aptamers targeting the PRV glycoprotein D (gD) through an optimized SELEX protocol. After 15 selection cycles, Apt-gD-2 demonstrated nanomolar affinity (Kd = 6.107 ± 0.476 nM) and high specificity for gD, as validated by an enzyme-linked aptamer-sorbent assay (ELASA) and fluorescence microscopy. Molecular docking revealed hydrogen bonding as the key interaction mechanism. The developed ic-ELASA achieved 83.3% concordance with qPCR in clinical samples, supporting its utility for on-farm PRV surveillance. These findings highlight the potential of aptamer-based diagnostic methods for rapid, sensitive, and onsite detection of PRV, offering a promising tool for disease control in the swine industry.

Keywords Aptamer, Pseudorabies virus, Glycoprotein D, ELASA, Viral diagnosis

Introduction

Pseudorabies (PRs), caused by the pseudorabies virus (PRV), are highly contagious and acute infectious diseases (Sun et al. 2023). Pigs are the natural hosts of PRV. Clinical manifestations vary with infection stage: fatal central nervous system disturbances are observed in piglets, adult pigs develop respiratory symptoms, and pregnant sows may experience abortion (Narita et al. 1994; Hsu et al. 1980). In addition to pigs, PRV can infect a wide range of animals, including cattle, sheep, cats, dogs, mink, and foxes (Salwa 2004; Jin et al. 2016; G.S. Wang et al. 2018). Notably, cases of PRV infection in farm workers have been documented, highlighting its zoonotic potential (Y. Wang et al. 2019; D. Wang et al. 2020).

PRV is an enveloped virus with a 143 kbp double-stranded DNA genome surrounded by a capsid, an envelope, and a tegument. The viral genome encodes 70–100 proteins, including ten glycoproteins that play critical roles in viral replication, immunogenicity, and pathogenicity. Among these, the gD glycoprotein binds to the cell surface receptor nectin-1, facilitating viral entry into host cells (Zheng et al. 2022; Pomeranz et al. 2005). Additionally, the gD protein is a key protective antigen for PRV and is capable of eliciting specific antibody responses in animals, making it a promising candidate for PRV recombinant subunit vaccines (Rue and Ryan 2003).

Early and rapid diagnosis of PRV infection is essential for its effective prevention and control. Current diagnostic methods include virus isolation, which is widely regarded as the "gold standard" owing to its high specificity and ability to detect live virus particles. PCR and RT-PCR are also commonly used for rapid detection and

Handling editor: Fang He.

*Correspondence:
Chao Zhang
chaozhang@henau.edu.cn
[1] College of Veterinary Medicine, Henan Agricultural University, Zhengzhou, Henan 450046, China
[2] Key Laboratory of Animal Growth and Development of Henan Province, Henan Agricultural University, Zhengzhou, Henan 450046, China
[3] Key Laboratory of Animal Biochemistry and Nutrition, Ministry of Agriculture and Rural Affairs, Zhengzhou, Henan 450046, China

differentiation between wild-type and vaccine strains of PRV (Ren et al. 2018). However, these techniques are often complex, require expensive equipment, and, particularly in the case of virus isolation, involve lengthy processing times. These limitations hinder their widespread application in the pig farming industry. Consequently, there is an urgent need for more cost-effective and time-efficient methods for PRV detection.

In recent years, aptamer-based rapid detection methods have been widely applied. Aptamers are single-stranded DNA or RNA molecules that fold into unique structures and bind specifically to their targets (Davydova et al. 2016; Nimjee et al. 2017). Aptamers are selected through the systematic evolution of ligands by the exponential enrichment (SELEX) process, and their targets can include proteins, viruses, bacteria, cells, or parasites (Gao et al. 2014; Morais et al. 2022; Ommen et al. 2022; Nagarkatti et al. 2014; Maradani et al. 2022; Nordin et al. 2024). Owing to their low cost, short production time, good stability, and ease of modification, aptamers have been widely used in diagnostic applications (Zou et al. 2019; Zhu et al. 2012; Tombelli et al. 2005).

The enzyme-linked immunosorbent assay (ELISA) is a well-established serological technique known for its simplicity, high sensitivity, and specificity (Ma et al. 2011). Several ELISA methods based on recombinant viral proteins have been developed for PRV detection (Shen et al. 2023; M. Guo et al. 2022; Gao et al. 2022). However, traditional ELISA relies on antibodies, which are costly to produce and require cold storage, limiting their practicality. In this study, we developed high-affinity, highly specific aptamers targeting the PRV gD protein and designed an indirect competitive enzyme-linked aptamer-sorbent assay (ic-ELASA), in which aptamers replace antibodies. This approach offers a cost-effective, user-friendly, and rapid diagnostic tool with significant potential for PRV detection in the field.

Results

Purification and identification of the maltose-binding protein (MBP)-gD fusion protein and the MBP tag protein

Previous studies have demonstrated that the extracellular domain of the PRV gD protein (amino acids 1–284) can be expressed in vitro in soluble form and can bindto the PRV receptor nectin-1 (Li et al. 2017). In this study, the 1-284 amino acid region of gD were ligated into the pET21b-His-MBP vector and expressed the recombinant protein in a prokaryotic expression system, which we designated MBP-gD. The SDS-PAGE analysis confirmed the purity of MBP-gD, showing a single band at ~ 75 kD and 45 kDa (Fig. 1A). To further confirm the identity of the purified MBP-gD recombinant protein, Western blot analysis was performed. The results revealed that both the purified MBP-gD protein and the MBP protein were able to bind with the MBP monoclonal antibody, yielding bands of the expected sizes (Fig. 1B). These findings demonstrate that the MBP-gD recombinant protein and the MBP tag protein were successfully prepared via the prokaryotic expression system.

Selection of DNA aptamers targeting the PRV gD protein

DNA aptamers targeting the gD protein were selected via the magnetic bead-based SELEX method. To increase the solubility of the gD protein, an MBP

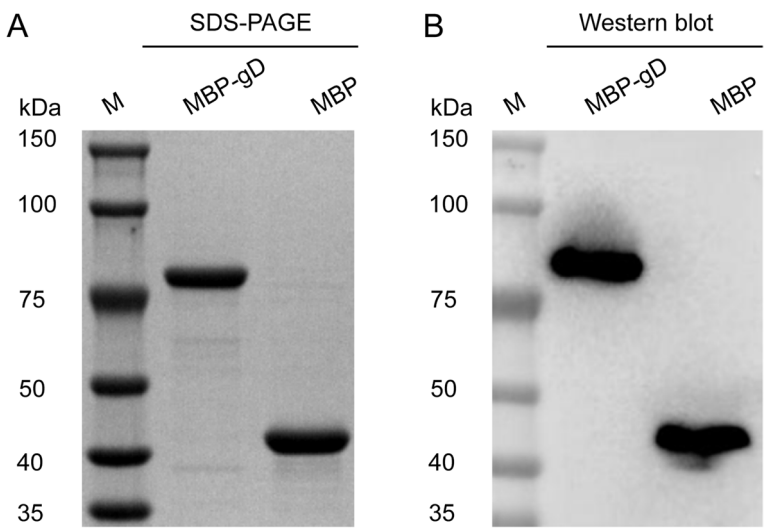

Fig. 1 Identification of the recombinant MBP-gD protein. **A** SDS-PAGE analysis of purified MBP-gD (75 kDa) and MBP (45 kDa) proteins. **B** Western blot analysis of the purified MBP-gD and MBP-tagged proteins. The primary antibody used was an MBP monoclonal antibody

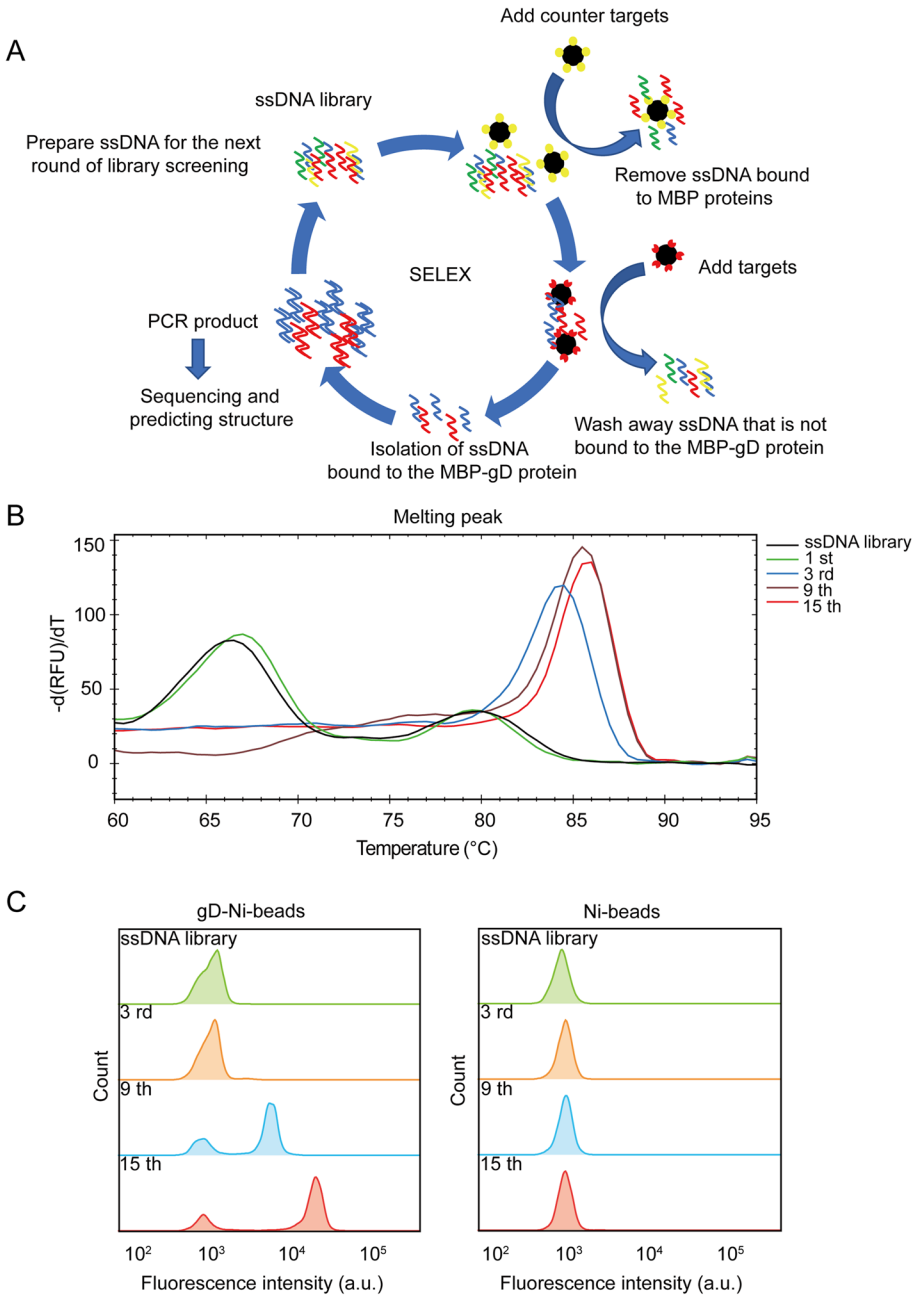

Fig. 2 Screening process and monitoring of DNA aptamers. **A** Flowchart of aptamer selection *via* the SELEX method. **B** qPCR analysis of ssDNA from rounds 1, 3, 9, and 15 to monitor library enrichment during selection. The initial random library served as a reference. **C** Flow cytometric analysis of FAM-labeled ssDNA libraries from rounds 3, 9, and 15 to assess binding to MBP-gD-conjugated magnetic beads. The unconjugated beads served as a negative control

solubility tag was fused to the N-terminus of gD. To eliminate the aptamers that nonspecifically bind to the MBP tag, negative selection was performed *via* the MBP tag protein during the screening process. A schematic representation of the screening procedure is provided in Fig. 2A.

The enrichment of DNA aptamers that bind to the gD protein was monitored *via* qPCR and flow cytometry. As the number of screening cycles increased, the melting temperature (Tm) observed via qPCR progressively increased, stabilizing at approximately 86 °C by the 15th round of selection. This indicated a reduction in library complexity and the successful enrichment of gD-binding

sequences (Fig. 2B). Flow cytometry analysis further revealed that the fluorescence intensity of the aptamers bound to the gD protein increased with each screening round, peaking after 15 rounds. In contrast, the control group with blank magnetic beads showed no significant fluorescence enhancement (Fig. 2C). These results confirmed the successful enrichment of DNA aptamers that specifically bind to the gD protein.

On the basis of these findings, the selection process was terminated after the 15th round. The single-stranded DNA (ssDNA) from the 15th round was PCR-amplified, inserted into the pMD18-T vector, and subjected to sequencing analysis. As shown in Table 1, the aptamers with the highest repeat frequency, Apt-gD-1 and Apt-gD-2, were selected as candidate aptamers for further experimental validation.

Evaluation of the binding affinity and specificity of DNA aptamers for the MBP-gD protein

The ability of the nucleic acid aptamers to bind to the MBP-gD protein was initially assessed via enzyme-linked aptamer-sorbent assay (ELASA). As the concentration of the nucleic acid aptamer increased, the binding affinity of Apt-gD-2 for the MBP-gD protein significantly increased, whereas Apt-gD-1 exhibited no detectable binding to the MBP-gD protein (Fig. 3A). Apt-gD-2 was selected for further characterization on the basis of these findings. The dissociation constant (Kd) of Apt-gD-2 binding to MBP-gD was determined to be 6.107 ± 0.476 nM (Fig. 3B).

The specificity of Apt-gD-2 binding to the gD protein was subsequently evaluated. ELASA confirmed that Apt-gD-2 specifically bound to the MBP-gD protein but did not bind to the MBP-S1, MBP-GP5, MBP, or BSA proteins (Fig. 3C). These results indicate that Apt-gD-2 is highly specific for the gD protein.

Secondary structure analysis of Apt-gD-2, performed via the online software Mfold, revealed that it forms a stable stem–loop structure (Fig. 3D). Furthermore, molecular docking analysis demonstrated that Apt-gD-2 interacts with the gD protein through hydrogen bonds, providing insights into the molecular basis of its binding specificity (Fig. 3E).

Evaluation of the binding of the aptamers to PRV virions

Biotinylated nucleic acid aptamers were refolded and incubated with purified PRV, PEDV, and PRRSV. ELASA results demonstrated that Apt-gD-2 selectively bound to PRV, whereas no significant binding was observed for PEDV or PRRSV (Fig. 4A). To further validate these findings, indirect immunofluorescence analysis was performed. The results confirmed that Apt-gD-2 specifically bound to PRV particles on the surface of infected cells (Fig. 4B). These data collectively indicate that Apt-gD-2 is highly specific for PRV virions.

Detection of PRV in tissue samples via indirect competitive ELASA

The indirect competitive enzyme-linked aptamer-sorbent assay (ic-ELASA) detection method is illustrated in Fig. 5A. To establish the critical value for this method, the OD450 values of 10 PRV-negative tissue samples were measured. The average percentage inhibition (PI) was calculated to be 11.83%, with a standard deviation of 4.839%. On the basis of these data, the critical value was set at 26.40%. Samples with PI values ≥ 26.40% were classified as positive, whereas those with PI values < 26.40% were classified as negative.

Next, the specificity of the ic-ELASA method was evaluated via the use of purified PRV, PEDV, and PRRSV. The results demonstrated that only PRV presented a PI value above the critical threshold of 26.40%, whereas PEDV and PRRSV presented PI values below this threshold (Fig. 5B). These findings confirm that the ic-ELASA method specifically detects the PRV. Furthermore, the lowest detectable amount of PRV was determined to be approximately $10^4 TCID_{50}$ (Fig. 5C), indicating the high sensitivity of this detection method.

Finally, the ic-ELASA method was applied to clinical tissue samples. As shown in Table 2, among the 30 samples analyzed, 17 (56.7%) were identified as PRVpositive, and 13 (43.3%) were PRVnegative. For comparison, conventional qPCR revealed that 20 (66.7%) samples were PRV positive and that 10 (33.3%) were PRV negative. The agreement rates between ic-ELASA and qPCR were 90% for negative results and 80% for positive results, with an overall agreement rate of 83.3%. These results demonstrate a high level of concordance between the ic-ELASA method and qPCR, highlighting the reliability of ic-ELASA for PRV detection.

Table 1 Candidate aptamer sequences

Name	Sequences (5′-3′)	Percentage
Apt-gD-1	AGTTGACGCTGGTGTGGGAC**ATGATTGTCGCCGTTTGAGGCCCATAGATCCGCAGGATGA**TCAATCTGCGTGCGTCCAGT	28.35%
Apt-gD-2	AGTTGACGCTGGTGTGGGAC**TTGGCGGGGGTGGGTTCTTTTGGTTTTACAGGGGGAGGGT**TCAATCTGCGTGCGTCCAGT	20.89%
Apt-gD-3	AGTTGACGCTGGTGTGGGAC**GGGGGTTTATGGTTACATATGCGTTAGGGGGGTGGGTGGT**TCAATCTGCGTGCGTCCAGT	8.95%

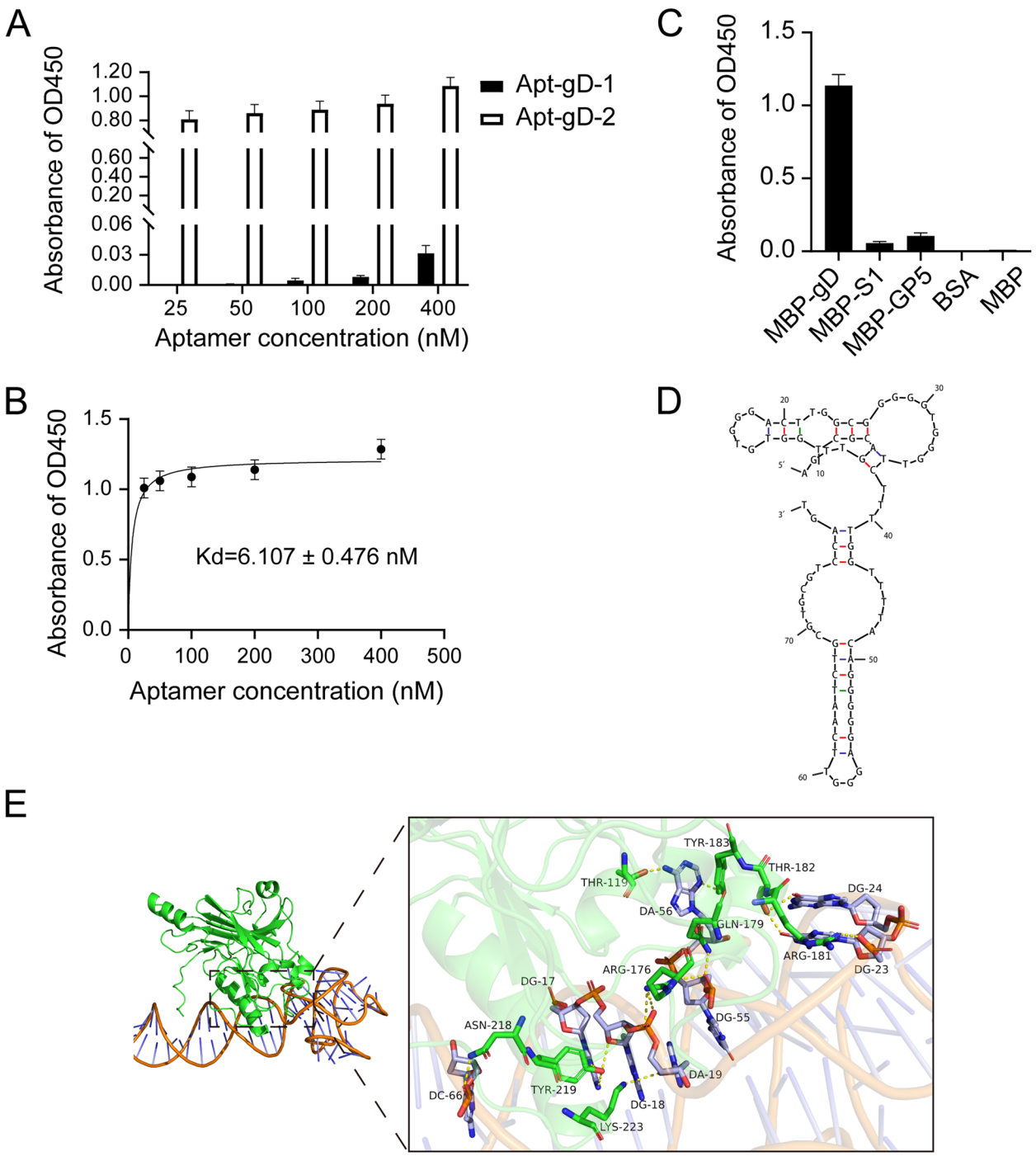

Fig. 3 ELASA detection of DNA aptamer affinity and specificity for the MBP-gD protein. **A** Detection of the affinity between biotin-labeled DNA aptamers and the MBP-gD protein at different concentrations (25, 50, 100, 200, and 400 nM) *via* ELASA. **B** Detection of the dissociation constant (Kd) of the aptamer by ELASA. Nonlinear curve fitting analysis was performed on the obtained data *via* Prism 8.0 to determine Kd of the DNA aptamer. **C** ELASA analysis of the specificity of aptamer binding to the MBP-gD protein. Biotinylated DNA aptamers (100 nM) were incubated with MBP-gD, MBP-S1, MBP-GP5, MBP, and BSA proteins. **D** The predicted secondary structure of the aptamer Apt-gD-2. **E** Molecular docking model of the aptamer Apt-gD-2 (orange) with the target protein gD (cyan). The yellow dashed lines indicate hydrogen bonds. The results are presented as the means ± SDs

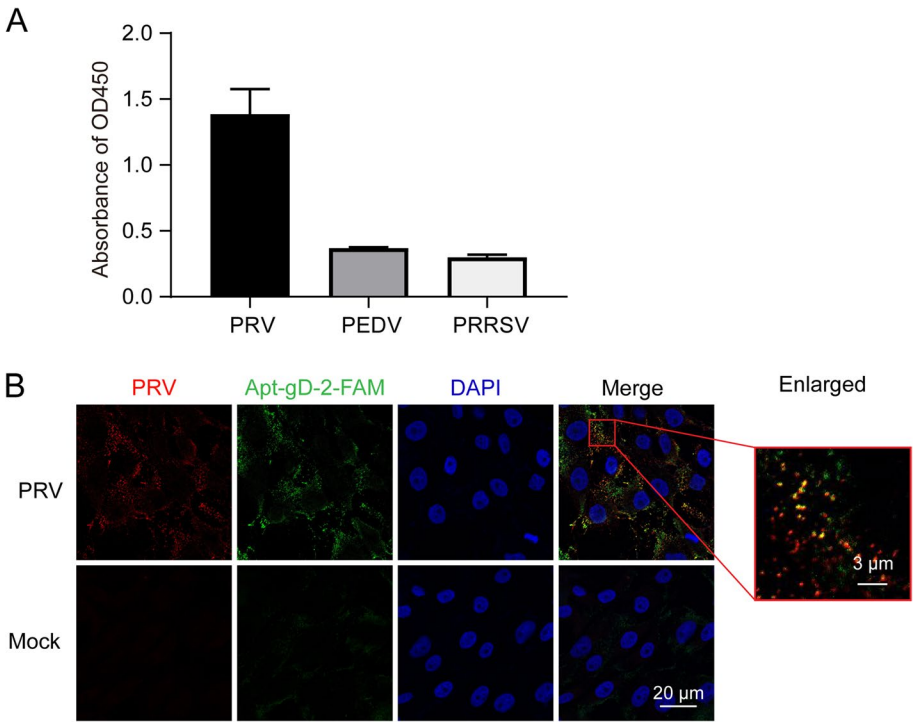

Fig. 4 Specific binding of DNA aptamers to PRV particles. **A** Binding of DNA aptamers to PRV, PEDV, and PRRSV viral particles was detected via ELISA. **B** Colocalization of FAM-labeled Apt-gD-2 with PRV-QXX-infected PK15 cells. Viral gB protein was detected via a mouse anti-gB mAb and Alexa Fluor® 594-labeled secondary antibody. Nuclei were stained with DAPI. A virus-free negative control was included. Images were captured via confocal microscopy

Discussion

PRV infection has caused significant economic losses to the global pig farming industry. Although the Bartha-K61 vaccine effectively controls the widespread transmission of PRV, the emergence of variant strains has compromised the protective efficacy of the vaccine, making early diagnosis a critical strategy for the prevention and control of PRV. Currently, diagnostic methods for PRV include virus isolation, PCR, qPCR, and ELISA (Zhou et al. 2022; Cheng et al. 2021; Z. Guo et al. 2024). While these methods are highly sensitive, their application in the field is limited because of their complexity, time-consuming procedures, high cost, and reliance on specialized equipment. Therefore, there is an urgent need to develop rapid, sensitive, and highly specific diagnostic methods that are easy to perform for the early detection and control of PRV.

ELISA is a well-established serological technique widely used for detecting PRV infection because of its sensitivity and efficiency (Zheng et al. 2021). ELISAs can be classified into direct, indirect, sandwich, and competitive formats (Aydin 2015). Competitive ELISA, also known as blocking ELISA, involves coating the antigen onto the plate and adding the antibody along with the sample. The concentration of the analyte in a sample is inversely proportional to the amount of antibody bound to the solid phase. The working principle of -ELASA is similar, except that the aptamers replace the antibodies. Aptamers offer several advantages over antibodies, including ease of synthesis through chemical methods, elimination of batch-to-batch variations (Toh et al. 2015), and dissociation constants that can reach the picomolar to femtomolar range (Cho et al. 2009; Gopinath and Kumar 2013). Additionally, as nucleic acids, aptamers can be readily labeled and modified with various molecules and functional groups (Luzi et al. 2003).

An ic-ELASA was developed for PRV detection by this research, in which PRV particles in the sample compete with the coated antigen MBP-gD protein for binding to the aptamer, enabling cost-effective detection of PRV. It demonstrated high sensitivity, with a minimum detectable concentration of approximately 10^4 $TCID_{50}$ for PRV. The effectiveness of ic-ELASA was further validated using clinical samples, showing an overall agreement rate of 83.3% compared to qPCR. Although qPCR is a widely used and highly sensitive method, it requires specialized personnel and is time-consuming due to its complex procedures. In contrast, ic-ELASA is easier to perform, making it a valuable complement to existing PRV detection methods.

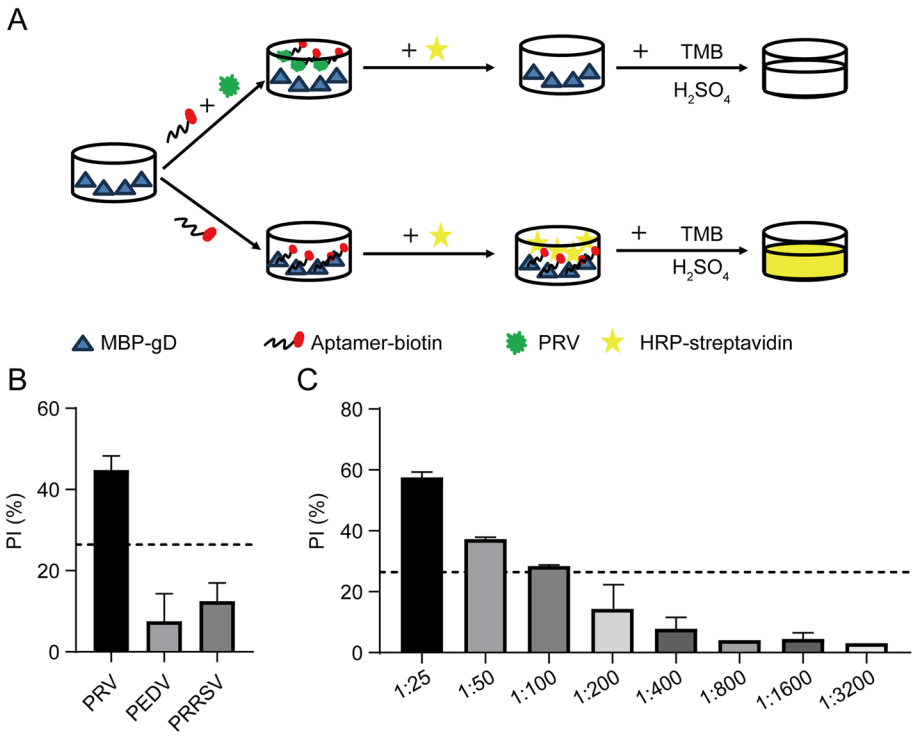

Fig. 5 Schematic representation and evaluation of the specificity and sensitivity of the indirect competitive enzyme-linked aptamer-sorbent assay (ic-ELASA). **A** Schematic of the ic-ELASA method. PRV competes with HRP-streptavidin for binding to biotinylated aptamers, enabling PRV detection. **B** Evaluation of the specificityof ic-ELASA for detecting purified PRV, PEDV, and PRRSV. The inhibition rate (PI) was calculated as follows: PI = [(OD450 of the negative control—OD450 of the test sample)/OD450 of the negative control] × 100%. **C** Sensitivity evaluation of the ic-ELASA method for PRV detection by performing twofold serial dilutions of PRV viral solution

Table 2 Clinical samples were detected by ic-ELASA and qPCR

	qPCR (+)	qPCR (-)	Total
ic-ELASA (+)	16	1	17
ic-ELASA (-)	4	9	13
Total	20	10	30

Conclusion

In this study, we developed high-affinity DNA aptamers targeting PRV gD, with Apt-gD-2 showing strong binding specificity. Based on this, an indirect competitive ELASA (ic-ELASA) was established, achieving high sensitivity (~ 10^4 $TCID_{50}$) and 83.3% agreement with qPCR. Compared to traditional methods, ic-ELASA is cost-effective, rapid, and user-friendly, making it ideal for on-site PRV detection in pig farms. These findings highlight the potential of aptamer-based diagnostics for PRV control and early detection.

Methods

Cells and reagents

Porcine kidney (PK-15) cells (CCL-33, ATCC) were cultured as a monolayer at 37°C with 5% CO_2 in Dulbecco's modified Eagle's medium (DMEM; 10,566–016, Gibco, Shanghai, China) supplemented with 10% fetal bovine serum (FBS; 10099141C, Gibco, Shanghai, China), 100 U/mL penicillin, and 100 μg/mL streptomycin sulfate (B540732, Sangon, Shanghai, China).

Prokaryotic expression and purification of PRV gD protein

The codon-optimized *gD* gene (NC_006151.1) was synthesized by GenScript (Nanjing, China) and cloned into the pET21b-His-MBP vector for prokaryotic expression. The construct was transformed into *Escherichia coli* BL21(DE3) cells, and protein expression was induced with 1 mM IPTG at 18°C overnight. The recombinant MBP-gD protein was purified *via* Ni–NTA affinity chromatography as previously described with minor modifications (Zhao et al. 2023). The protein concentration was measured via a BCA protein assay kit (DingGuo, Beijing, China), and its purity and identity were confirmed via SDS–PAGE and western blot analysis.

Screening and identification of DNA aptamers that target the MBP-gD protein

The screening process for DNA aptamers was carried out as previously described with minor modifications (Song

et al. 2020). A random ssDNA library was synthesized by GeneScript, which contained two fixed 20-base primer regions and a 40-base random region 5'-AGTTGACGC TGGTGTGGGAC-N40-TCAATCTGCGTGCGTCCA GT-3'). Five nanomoles of the library were denatured, cooled, and equilibrated before incubation with MBP-gD-coated Ni magnetic beads at room temperature for 30 min. After washing, bound sequences were eluted and amplified *via* PCR with the primers 5'-FAM-AGTTGA CGCTGGTGTGGGAC-3' and 5'-Phosphate-ACTGGA CGCACGCAGATTGA-3'. Single-stranded DNA was obtained *via* Lambda exonuclease digestion. The negative selection with MBP-coated beads was introduced from the fourth round.

The qPCR was performed to monitor enrichment at the 1st, 3rd, 9th, and 15th rounds, and the flow cytometry was used to evaluate binding affinity. The final selected ssDNA pool was cloned into the pMD18-T vector and sequenced (Tsingke Biotechnology, Beijing, China). The secondary structures of the aptamers were predicted via the online tool Mfold (http://www.unafold.org/).

Enzyme-linked aptamer-sorbent assay (ELASA)

Purified MBP-gD protein or virus was coated onto an ELISA plate (100 μL/well), followed by washing with PBST and blocking with 1% BSA for 1 h. Biotinylated aptamers were denatured at 95°C, cooled, equilibrated, and added to the wells for a 1-h incubation. After washing, HRP-conjugated streptavidin (1:10,000) was added and incubated for one hour. The reaction was developed using TMB substrate, stopped with acid, and the absorbance was measured at 450 nm *via* a microplate reader.

Molecular docking of DNA aptamers with the gDprotein

The 3D structures of the DNA aptamers were modeled *via* AlphaFold 3, whereasthe target protein gD was homology-modeled by SWISS-MODEL (https://swissmodel.expasy.org/). Molecular docking simulations were performed via the HDOCK server (http://hdock.phys.hust.edu.cn/). The interactions between the DNA aptamers and gD protein were visualized using PyMOL.

Indirect immunofluorescence detection of DNA aptamer binding to PRV

PK-15 cells were cultured in 24-well plates with coverslips. After cell counting, the cells were infected with PRV-QXX (MOI = 0.05) at 4°C for 1 h. A control group without virus was included. The cells were incubated with 500 nM Apt-gD-2-FAM for 1 h at room temperature. Fixed cells were permeabilized and blocked, followed by staining with PRV gB monoclonal antibody and Alexa Fluor 594® goat anti-mouse IgG (Thermo Fisher, Shanghai, China) for indirect immunofluorescence.

Detection of PRV in pig tissue samples

A total of thirty clinical tissue samples stored in our laboratory were processed. Lymph nodes, the spleen, and other tissues from pigs suspected of being infected with PRV were collected and minced. A 0.1 g sample of tissue was then added to 1 mL of PBS containing 0.55 mmol/L $MgCl_2$ and homogenized. The homogenate underwent three freeze–thawcycles at −80°C, followed by centrifugation at 4°C for 30 min at 10,000 rpm. The resulting supernatant was collected and used as the sample for further analysis.

Viral genomic DNA was extracted from the tissue supernatants *via* a viral genomic extraction kit (SangonBiotech, Shanghai, China). The samples were subsequently tested via both qPCR and ic-ELASA. The concordance between the results of these two methods was calculated to assess the consistency and reliability of the detection.

Acknowledgements

We are grateful to Professor Yongtao Li (Henan Agricultural University) for providing PRV strain (PRV-QXX), PRRSV strain (PRRSV SD16) and PEDV strain (PEDV-HW).

Authors' contributions

Zhihao Wang and Yan Qiao: conceptualization, investigation, methodology, and writing original draft. Jiafu Zhao, Xiaotian Chang and Heshui Zhu: methodology andsample preparation. Chao Zhang: conceptualization,supervision, review, and editing. Zhihao Wang and Yan Qiao contributed equally to this work.

Funding

This work was supported by the Henan Provincial Science and Technology Research Project (Grant No. 242102110019) and the National Natural Science Foundation of China (Grant No. 31972672).

Data availability

The datasets used and/or analyzed during the current study are available from the corresponding author on reasonable request.

Declarations

Ethics approval and consent to participate

This study involved the use of pig tissue samples for the detection of PRV. The research was approved by the Animal Ethics Committee of Henan Agricultural University. All experimental procedures were conducted in strict accordance with animal welfare regulations, and efforts were made to minimize the pain and discomfort of the animals.

Consent for publication

Not applicable.

Competing interests

The authors declare no competing interests.

Received: 25 January 2025 Accepted: 13 March 2025
Published online: 07 April 2025

References

Aydin, S. 2015. A short history, principles, and types of ELISA, and our laboratory experience with peptide/protein analyses using ELISA. *Peptides* 72: 4–15. https://doi.org/10.1016/j.peptides.2015.04.012.

Cheng, T.Y., A. Henao-Diaz, K. Poonsuk, A. Buckley, A. van Geelen, K. Lager, K. Harmon, P. Gauger, C. Wang, A. Ambagala, J. Zimmerman, and L. Giménez-Lirola. 2021. Pseudorabies (Aujeszky's disease) virus DNA detection in swine nasal swab and oral fluid specimens using a gB-based real-time quantitative PCR. *Preventive Veterinary Medicine* 189: 105308. https://doi.org/10.1016/j.prevetmed.2021.105308.

Cho, E.J., J.W. Lee, and A.D. Ellington. 2009. Applications of aptamers as sensors. *Annu Rev Anal Chem (Palo Alto Calif)* 2: 241–264. https://doi.org/10.1146/annurev.anchem.1.031207.112851.

Davydova, A., M. Vorobjeva, D. Pyshnyi, S. Altman, V. Vlassov, and A. Venyaminova. 2016. Aptamers against pathogenic microorganisms. *Critical Reviews in Microbiology* 42 (6): 847–865. https://doi.org/10.3109/1040841x.2015.1070115.

Gao, Y., X. Yu, B. Xue, F. Zhou, X. Wang, D. Yang, N. Liu, L. Xu, X. Fang, and H. Zhu. 2014. Inhibition of hepatitis C virus infection by DNA aptamer against NS2 protein. *PLoS ONE* 9 (2): e90333. https://doi.org/10.1371/journal.pone.0090333.

Gao, Y., T. Xia, J. Bai, L. Zhang, H. Zheng, and P. Jiang. 2022. Preparation of monoclonal antibodies against the viral p54 protein and a blocking ELISA for detection of the antibody against African swine fever virus. *Viruses* 14(11). https://doi.org/10.3390/v14112335.

Gopinath, S.C., and P.K. Kumar. 2013. Aptamers that bind to the hemagglutinin of the recent pandemic influenza virus H1N1 and efficiently inhibit agglutination. *Acta Biomaterialia* 9 (11): 8932–8941. https://doi.org/10.1016/j.actbio.2013.06.016.

Guo, M., S. Du, L. Lai, W. Wu, X. Huang, A. Li, H. Li, C. Li, Q. Wang, L. Sun, et al. 2022. Development and evaluation of recombinant E2 protein based IgM capture enzyme-linked immunosorbent assay (ELISA) and double antigen sandwich ELISA for detection of antibodies to Chikungunya virus. *PLoS Neglected Tropical Diseases* 16 (12): e0010829. https://doi.org/10.1371/journal.pntd.0010829.

Guo, Z., H. Xu, S. Zhang, H. Kang, C. Li, Q. Sun, J. Zhao, J. Li, G. Zhou, Q. Wang, et al. 2024. Improved detection sensitivity of anti-PRV variant antibodies through preparation of anti-gB and anti-gE monoclonal antibodies and development of blocking ELISAs. *International Journal of Biological Macromolecules* 260 (Pt 1): 129425. https://doi.org/10.1016/j.ijbiomac.2024.129425.

Hsu, F.S., R.M. Chu, R.C. Lee, and S.H. Chu. 1980. Placental lesions caused by pseudorabies virus in pregnant sows. *Journal of the American Veterinary Medical Association* 177 (7): 636–641.

Jin, H.L., S.M. Gao, Y. Liu, S.F. Zhang, and R.L. Hu. 2016. Pseudorabies in farmed foxes fed pig offal in Shandong province, China. *Archives of Virology* 161 (2): 445–448. https://doi.org/10.1007/s00705-015-2659-9.

Li, A., G. Lu, J. Qi, L. Wu, K. Tian, T. Luo, Y. Shi, J. Yan, and G.F. Gao. 2017. Structural basis of nectin-1 recognition by pseudorabies virus glycoprotein D. *PLoS Pathogens* 13 (5): e1006314. https://doi.org/10.1371/journal.ppat.1006314.

Luzi, E., M. Minunni, S. Tombelli, and M. Mascini. 2003. New trends in affinity sensing: Aptamers for ligand binding. *Trac Trends in Analytical Chemistry* 22 (11): 810–818.

Ma, L.N., J. Zhang, H.T. Chen, J.H. Zhou, Y.Z. Ding, and Y.S. Liu. 2011. An overview on ELISA techniques for FMD. *Virol J* 8: 419. https://doi.org/10.1186/1743-422x-8-419.

Maradani, B.S., S. Parameswaran, and K. Subramanian. 2022. Development and characterization of DNA aptamer against Retinoblastoma by Cell-SELEX. *Science and Reports* 12 (1): 16178. https://doi.org/10.1038/s41598-022-20660-3.

Morais, L. M., T. S. Chaves, M. A. Medeiros, K. A. B. Pereira, P. B. Jurgilas, S. M. Barbosa de Lima, S. Missailidis, and A. M. Bispo de Filippis. 2022. Selection and characterization of single-stranded DNA aptamers of diagnostic potential against the whole Zika virus. *Viruses* 14(9). https://doi.org/10.3390/v14091867.

Nagarkatti, R., F.F. de Araujo, C. Gupta, and A. Debrabant. 2014. Aptamer based, non-PCR, nonserological detection of Chagas disease biomarkers in Trypanosoma cruzi infected mice. *PLoS Neglected Tropical Diseases* 8 (1): e2650. https://doi.org/10.1371/journal.pntd.0002650.

Narita, M., K. Kawashima, S. Matsuura, A. Uchimura, and Y. Miura. 1994. Pneumonia in pigs infected with pseudorabies virus and Haemophilus parasuis serovar 4. *Journal of Comparative Pathology* 110 (4): 329–339. https://doi.org/10.1016/s0021-9975(08)80310-6.

Nimjee, S.M., R.R. White, R.C. Becker, and B.A. Sullenger. 2017. Aptamers as therapeutics. *Annual Review of Pharmacology and Toxicology* 57:61–79. https://doi.org/10.1146/annurev-pharmtox-010716-104558.

Nordin, N.A., S. Soon, J.B. Senawi, Z.A.M. Jinin, S.S. Arshad, A.R. Yasmin, and F.A. Azri. 2024. Aptamer-based detection of foot-and-mouth disease virus using single-stranded DNA probe. *Applied Biochemistry and Biotechnology*. https://doi.org/10.1007/s12010-024-05093-0.

Ommen, P., L. Hansen, B.K. Hansen, H. Vu-Quang, J. Kjems, and R.L. Meyer. 2022. Aptamer-targeted drug delivery for *Staphylococcus aureus* biofilm. *Frontiers in Cellular and Infection Microbiology* 12:814340. https://doi.org/10.3389/fcimb.2022.814340.

Pomeranz, L.E., A.E. Reynolds, and C.J. Hengartner. 2005. Molecular biology of pseudorabies virus: Impact on neurovirology and veterinary medicine. *Microbiology and Molecular Biology Reviews* 69 (3): 462–500. https://doi.org/10.1128/mmbr.69.3.462-500.2005.

Ren, M., H. Lin, S. Chen, M. Yang, W. An, Y. Wang, C. Xue, Y. Sun, Y. Yan, and J. Hu. 2018. Detection of pseudorabies virus by duplex droplet digital PCR assay. *Journal of Veterinary Diagnostic Investigation* 30 (1): 105–112. https://doi.org/10.1177/1040638717743281.

Rue, C.A., and P. Ryan. 2003. A role for glycoprotein C in pseudorabies virus entry that is independent of virus attachment to heparan sulfate and which involves the actin cytoskeleton. *Virology* 307 (1): 12–21. https://doi.org/10.1016/s0042-6822(02)00024-7.

Salwa, A. 2004. A natural outbreak of Aujeszky's disease in farm animals. *Polish Journal of Veterinary Sciences* 7 (4): 261–266.

Shen, Z., W. Qiu, H. Luan, C. Sun, X. Cao, G. Wang, and J. Peng. 2023. I329L protein-based indirect ELISA for detecting antibodies specific to African swine fever virus. *Frontiers in Cellular and Infection Microbiology* 13: 1150042. https://doi.org/10.3389/fcimb.2023.1150042.

Song, Y., J. Song, X. Wei, M. Huang, M. Sun, L. Zhu, B. Lin, H. Shen, Z. Zhu, and C. Yang. 2020. Discovery of aptamers targeting the receptor-binding domain of the SARS-CoV-2 spike glycoprotein. *Analytical Chemistry* 92 (14): 9895–9900. https://doi.org/10.1021/acs.analchem.0c01394.

Sun, Y.M., C. Li, Z.Z. Liu, W. Zeng, M.J. Ahmad, M.J. Zhang, L.N. Liu, S.J. Zhang, W.T. Li, and Q.G. He. 2023. Chinese herbal extracts with antiviral activity: evaluation, mechanisms, and potential for preventing PRV. *PEDV and PRRSV Infections. Animal Diseases.* 3: 35. https://doi.org/10.1186/s44149-023-00091-x.

Toh, S.Y., M. Citartan, S.C. Gopinath, and T.H. Tang. 2015. Aptamers as a replacement for antibodies in enzyme-linked immunosorbent assay. *Biosensors & Bioelectronics* 64: 392–403. https://doi.org/10.1016/j.bios.2014.09.026.

Tombelli, S., M. Minunni, and M. Mascini. 2005. Analytical applications of aptamers. *Biosensors & Bioelectronics* 20 (12): 2424–2434. https://doi.org/10.1016/j.bios.2004.11.006.

Wang, G.S., Y. Du, J.Q. Wu, F.L. Tian, X.J. Yu, and J.B. Wang. 2018. Vaccine resistant pseudorabies virus causes mink infection in China. *BMC Veterinary Research* 14 (1): 20. https://doi.org/10.1186/s12917-018-1334-2.

Wang, Y., H. Nian, Z. Li, W. Wang, X. Wang, and Y. Cui. 2019. Human encephalitis complicated with bilateral acute retinal necrosis associated with pseudorabies virus infection: A case report. *International Journal of Infectious Diseases* 89: 51–54. https://doi.org/10.1016/j.ijid.2019.09.019.

Wang, D., X. Tao, M. Fei, J. Chen, W. Guo, P. Li, and J. Wang. 2020. Human encephalitis caused by pseudorabies virus infection: A case report. *Journal of Neurovirology* 26 (3): 442–448. https://doi.org/10.1007/s13365-019-00822-2.

Zhao, M., J. Chen, S. Luo, R. Yan, P. Zhang, Z. Ren, X. Chen, G. Wang, H. Xiang, R. Cai, Y. Huang, N. Li, H. Li, Z.G. Yuan, and X. Wang. 2023. Pseudorabies gD protein protects mice and piglets against lethal doses of pseudorabies virus. *Frontiers in Microbiology* 14: 1288458. https://doi.org/10.3389/fmicb.2023.1288458.

Zheng, H.H., Y. Jin, C.Y. Hou, X.S. Li, L. Zhao, Z.Y. Wang, and H.Y. Chen. 2021. Seroprevalence investigation and genetic analysis of pseudorabies virus within pig populations in Henan province of China during 2018–2019. *Infection, Genetics and Evolution* 92: 104835. https://doi.org/10.1016/j.meegid.2021.104835.

Zheng, H. H., P. F. Fu, H. Y. Chen, and Z. Y. Wang. 2022. Pseudorabies virus: From pathogenesis to prevention strategies. *Viruses* 14(8). https://doi.org/10.3390/v14081638.

Zhou, Q., L. Zhang, H. Liu, G. Ye, L. Huang, and C. Weng. 2022. Isolation and characterization of two pseudorabies virus and evaluation of their effects on host natural immune responses and pathogenicity. *Viruses* 14(4). https://doi.org/10.3390/v14040712.

Zhu, G., M. Ye, M.J. Donovan, E. Song, Z. Zhao, and W. Tan. 2012. Nucleic acid aptamers: An emerging frontier in cancer therapy. *Chemical Communications (Cambridge, England)* 48 (85): 10472–10480. https://doi.org/10.1039/c2cc35042d.

Zou, X., J. Wu, J. Gu, L. Shen, and L. Mao. 2019. Application of aptamers in virus detection and antiviral therapy. *Frontiers in Microbiology* 10:1462. https://doi.org/10.3389/fmicb.2019.01462.

Publisher's Note